

Numerical Test of Born-Oppenheimer Approximation in Chaotic Systems

Jeong-Bo Shim¹, Mahir S. Hussein^{1,2}, and Martina Hentschel¹

¹Max-Planck Institute for the Physics of Complex Systems, Nöthnitzer Str. 38, Dresden, Germany

²Instituto de Física, Universidade de São Paulo, C.P. 66318, São Paulo, SP, Brazil

(Dated: November 17, 2018)

We study the validity of the Born-Oppenheimer approximation in chaotic dynamics. Using numerical solutions of autonomous Fermi accelerators, we show that the general adiabatic conditions can be interpreted as the narrowness of the chaotic region in phase space.

PACS numbers:

I. INTRODUCTION

The Born-Oppenheimer approximation is a method which deals with a coupled system of heavy and light objects[1]. From atomic physics to nuclear physics, it has played an important role. Moreover, the importance of this method gets greater as the necessity of the adiabatic control of quantum states arises in the quantum information science[2].

Nevertheless, the criteria of the validity of the method is not well defined yet, even still controversial in some aspects[3, 4]. Therefore, more theoretical work is needed through applications to specific models.

In this paper, we focused on the effect of chaotic dynamics in the Born-Oppenheimer approximation method. Since the Born-Oppenheimer approximation basically deals with coupled systems, there is always the possibility of non-integrability generating chaotic dynamics[5]. For this study, we choose the Fermi accelerator as a model of Hamiltonian chaos[6].

Originally, the Fermi accelerator has been proposed to explain the origin of fast cosmic rays and developed further by Ulam[7]. However, this model has had more importance as a standard Hamiltonian system to exhibit chaotic dynamics. Because of its simple composition and yet rich dynamics, it has been intensely studied both classically[5, 8] and quantum mechanically[9, 10, 11]. The feature of harmonically driven barriers is frequently encountered in various physical situations[12, 13], hence it provides very useful physical insights in spite of its simple structure. Furthermore, physical features of the model have been realized experimentally in an atomic system[14].

Besides the considerations of various regimes, several varieties of the Fermi accelerator have also been proposed, including relativistic models, of the type which embodies thermodynamic considerations[15] and mechanical Fermi accelerator with damping[16]. Our model can however be contrasted with the previous ones in terms of energy conservation. While the general Fermi accelerator has a periodic external driving force, the two moving objects in our system simply exchange energy with each other, but always maintaining the total energy conserved. (In the relativistic regime, the system

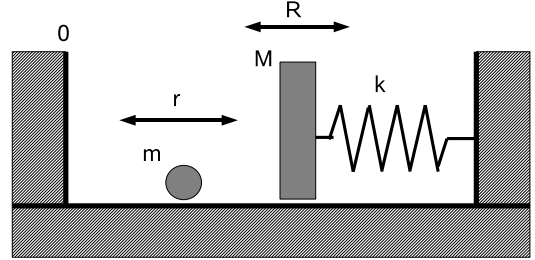


FIG. 1: Schematic diagram of the autonomous Fermi accelerator

can have a constant energy effectively in spite of the driving, but it is conditionally given. See [15]) Accordingly, this model may be called an ‘Autonomous Fermi Accelerator’(AFA), and the property of energy conservation enables us to calculate the exact eigenstates. With this set of eigenstates, we analyze the dynamics of the AFA and derive the condition for the validity of the Born-Oppenheimer approximation in the chaotic regime.

This paper is organized as following. In Sec. II, we describe the autonomous Fermi accelerator schematically and present the analysis of its classical dynamics by phase space portraits. The phase space of the system shows under what conditions the chaotic dynamics sets in. Then we apply the Born-Oppenheimer approximation to the system in Sec. III. We then compare the approximated calculation with the exact numerical solution which is obtained in Sec. III. Through this comparison, the connection between the conventional criteria of the Born-Oppenheimer approximation and the chaotic dynamics can be derived.

II. CLASSICAL DYNAMICS

The autonomous Fermi accelerator consists of a free particle confined between two infinite potential barriers. Both barriers are not penetrable and one of them has a finite mass and moves in a harmonic potential, while the other one is fixed. The schematical description is shown

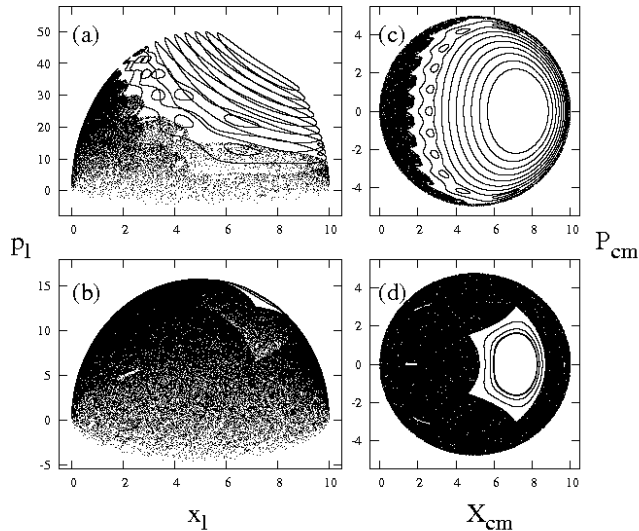


FIG. 2: Phase space portraits of the autonomous Fermi accelerator. The plots are constructed by recording dynamical phases at each collision between the light particle and the heavy wall : (a), (b) Plots of dynamical phases of a light particle. (c), (d) Same plots of a center of masses. The mass ratio(η) and the total energy(E) for each plot are assigned as ($\eta = 0.01$, $E = 12.0$) for (a) and (c), and ($\eta = 0.1$, $E = 12.0$) for (b) and (d).

in Fig. 1.

The Hamiltonian of the autonomous Fermi accelerator is given by

$$H(P, p, R, r) = \frac{P^2}{2M} + \frac{p^2}{2m} + \frac{1}{2}k^2(R - R_0)^2, \quad (1)$$

where M , P and R are a mass, momentum and position variable for the oscillating heavy wall, while m , p and r are those for the free particle. We set the fixed wall at $R = 0$ and the minimum point of the harmonic potential at $R_0 = 5$. Also, we assume that every collision between the particle and the wall is elastic.

First, we analyze the classical dynamics of this system by Poincare surface of sections. The surface of section can be constructed stroboscopically by sampling the dynamical status of either the particle or the wall at each collision. The obtained results with different parameters are presented in Fig. 2. The right column of the figure shows the phase space plots of the light particle and the left one shows those of the center of masses.

In this figure, we can notice that the feature of energy conservation is vividly shown; namely that all dynamical phases are restricted on a spherical surface given by

$$E = \frac{P^2}{2M} + \frac{p^2}{2m} + \frac{1}{2}k^2(R - R_0)^2. \quad (2)$$

As Fig. 2 shows, the phase space of the system is quite clearly divided into two parts, a stochastic and a regular part. The border between them is conditioned by the existence of the double collision. Here, the double collision means the situation that the light particle is hit by the heavy wall twice until it reaches the fixed wall. The presence of this type of collision diverges the light particle's trajectory drastically, and results in the stochastic dynamics. Apparently, it can be a necessary condition for the double collision that the heavy wall is faster than the light particle. Fig. 2 shows such tendency well. The stochastic region is located around the equator of the sphere in the phase space, while the regular island is around the pole.

We also mention a structural detail in phase space: Around the border between the chaotic and the regular region there exists "Stochastic Web Structure" [17]. However, this structure is ignorable in the regime of wave mechanical parameters in this study.

The structural properties of the phase space, including the portion of the regular and chaotic region, is controlled mainly by the mass ratio(η). By the comparison of (a) and (b) in Fig. 2, we can confirm the tendency that the regular island is shrunk as η is increased. Also the phase space is affected by the total energy(E), but the portion of regular island is not changed as much as by the mass ratio, according to our numerical study.

III. BORN-OPPENHEIMER APPROXIMATION

If the system is quantized, the total Hamiltonian becomes

$$H = -\frac{\hbar^2}{2M} \frac{\partial^2}{\partial R^2} - \frac{\hbar^2}{2m} \frac{\partial^2}{\partial r^2} + \frac{1}{2}k(R - R_0)^2 \quad (3)$$

and the Schrödinger equation and the boundary condition are given by

$$H\Psi(r, R) = E\Psi(r, R), \quad (4)$$

$$\Psi(r = 0, R) = \Psi(R \leq r, r) = 0. \quad (5)$$

Application of the Born-Oppenheimer approximation means to fix all parameters which are given instantaneously by the heavy object. In our system, this can be done by fixing the distance between the walls, to be R , at every moment. Then, a set of basis states can be constructed as follows:

$$\Psi(R, r) = \sum_n \xi_n(R) \phi_n(r, R) \quad (6)$$

where

$$\phi_n(r, R) = \sqrt{\frac{2}{R}} \sin \frac{n\pi r}{R}. \quad (7)$$

Using the completeness of the basis set above, the Schrödinger equation (4) can be reduced in the following way:

$$\sum_{n'} \langle \phi_n | -\frac{1}{2M} \frac{\partial^2}{\partial R^2} | \phi_{n'} \rangle \xi_{n'}(R) + \frac{1}{2} k(R - R_0)^2 \xi_n(R) + \epsilon_n \xi_n(R) = E \xi_n(R), \quad (8)$$

where $\epsilon = (\hbar n \pi)^2 / 2mR^2$.

If Eq. (7) is inserted into (8), one is able to expand the equation with the mass-ratio, $\eta (= m/M)$ as a parameter. By taking up to the first order of this expansion, the following equation is obtained,

$$\begin{aligned} \left(-\eta \frac{\partial^2}{\partial R^2} + \eta \frac{Mk}{\hbar^2} (R - R_0)^2 - \frac{n^2 \pi^2}{R^2} \right) \xi_n(R) \\ = \eta \frac{2ME}{\hbar^2} \xi_n(R). \end{aligned} \quad (9)$$

Consequently, the governing equation is reduced to a simple 1-dimensional equation of motion with a stationary bounding potential and the third term of the equation can be thought of as a pressure generated by the frequent collisions of the light particle.

According to the theory of Hamiltonian chaos, there is no possibility of chaos if we consider the dynamics at the pure classical level. However, if we take the level transition into account, the effective potential can be thought of to be time-dependent, and it seems more reasonable as the counterpart of the classical chaotic system. Along this line of reasoning, if an eigenmode is corresponding to chaotic dynamics, we can make an assumption that the lowest order of approximation would fail to describe the eigenmode. The validity of this assumption, will be discussed in the next section through a discussion of the exact solution which is numerically obtained.

IV. NUMERICAL STUDY

As mentioned in the introduction, the exact solutions of the system are also available. To calculate them, the following transform is performed.

$$R = x, \quad r = \eta y. \quad (10)$$

Then the Schrödinger equation becomes

$$\left(-\frac{\hbar^2}{2M} \nabla^2 + \frac{1}{2} k(x - x_0)^2 \right) \Psi(x, y) = E \Psi(x, y). \quad (11)$$

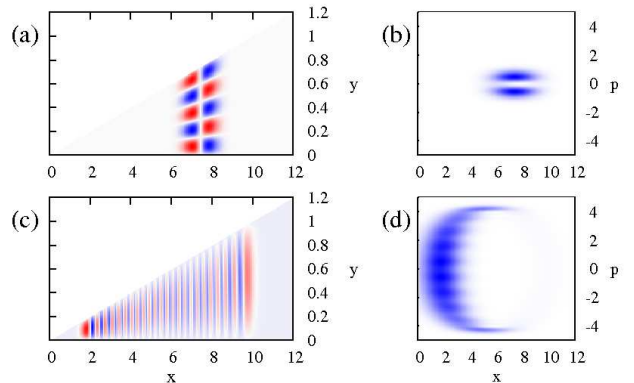


FIG. 3: Configurational Plots of Eigenmodes at $\eta = 0.01$. : (a) Regular mode : $E = 12.38$ (c) Chaotic mode : $E = 12.29$. (b), (d) : Corresponding Husimi distributions to (a) and (c), respectively

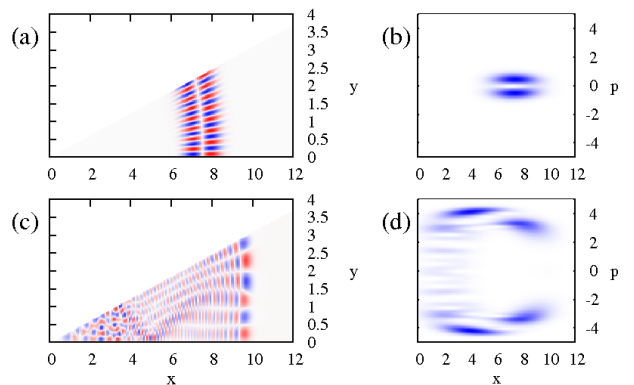


FIG. 4: Configurational Plots of Eigenmodes at $\eta = 0.1$: (a) Regular mode : $E = 12.22$ (c) Chaotic mode : $E = 12.19$. (b), (d) : Corresponding Husimi distributions to (a) and (c), respectively.

As the result of the transformation, the 1-dimensional dynamics of the system becomes a 2-dimensional dynamics in a triangular well, the three sides of which are two infinite potential barriers along the x-axis and $y = \tan \theta x$, and one harmonic potential barrier to the x-direction. Here, the angle θ between the two infinite barriers is given by

$$\theta = \tan^{-1} \sqrt{\eta}, \quad (12)$$

where η is the mass ratio ($= m/M$). It should be noted

that θ would reach $\pi/2$ as η approaches infinity. In this work, we are concerned only with the normal situation of Born-Oppenheimer approximation, namely that M is much larger than m .

Then the boundary condition is given as

$$\begin{aligned}\Psi(x, y = 0) &= 0, \\ \Psi(x, y = \tan \theta x) &= 0, \\ \Psi(x \rightarrow \infty, y) &= 0.\end{aligned}\quad (13)$$

Using a numerical approach, we obtain all possible eigenvalues and corresponding eigenmodes with two different mass-ratio parameters, $\eta = 0.01$ and 0.1 . As the numerical algorithm, ‘Finite Element Method’[18] is used.

Fig. 3 and Fig. 4 show configurational plots and Husimi distributions of eigenmodes at $\eta = 0.01$ and $\eta = 0.1$, respectively. Using the normal derivative of configurational mode distributions along $y = \eta x$, we can calculate the Husimi distributions, and these are corresponding to the Poincarè surface of section of a center of mass. Hence, the corresponding dynamics for each mode can be confirmed by comparison of the Husimi distributions with the classical phase spaces in Fig. 2. In Fig. 3 and 4, (a) and (b) of each figure shows a mode which is localized the regular regime in the phase space, and (c) and (d) shows ones in the chaotic regime.

From the obtained computational results, the validity of the Born-Oppenheimer approximation is investigated. For this purpose, the Fourier analysis is performed to find the eigenmode composition of the light particle.

$$F(n) = \int_0^\infty \int_0^{\eta x} \Psi(x, y) \sin(n\pi y/x) dy dx \quad (14)$$

The result of the analysis shows the different features of distributions, depending on the underlying dynamics. For $\eta = 0.01$, the distribution is well localized regardless to the dynamics (see Fig. 5(a)). For $\eta = 0.1$, however, the distribution shows the interesting features depending on the dynamics (Fig. 5(b)). The mode which is placed in the chaotic region shows a broad distribution, with tails reaching the regular region, but the one in the regular region still has a well localized distribution.

Considering the scheme of the Born-Oppenheimer approximation, modes with the high localization are expected to be well-approximated. To confirm this, we extract the wave function of the moving wall with the highest level (\bar{n}) in each distribution in the following way,

$$\psi(x) = \int_0^\infty \Psi(x, y) \sin(\bar{n}\pi y/x) dy. \quad (15)$$

Fig. 5 presents a comparison between the wave function extracted from the exact wave function in Fig. 3(c)

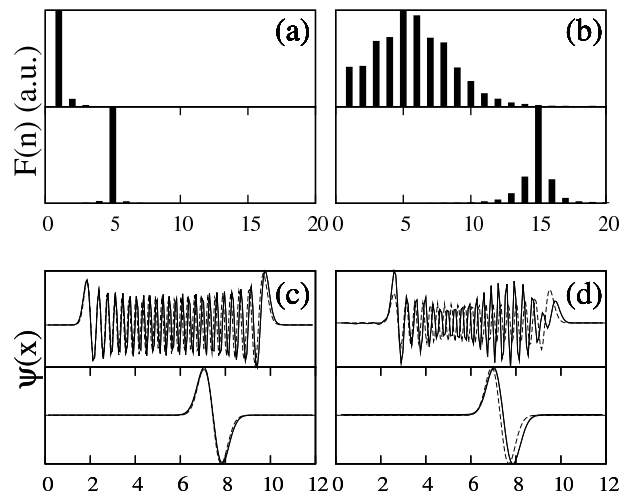


FIG. 5: (a) The analysis of the modes in Fig. 3 ($\eta = 0.01$) under the instantaneous basis of the light particle. (b) The same one for Fig. 4. In each figure, the upper distribution is for modes in the chaotic region and the lower one is for ones in the regular region. (c), (d) The extracted wave functions of the moving wall (solid line) and the approximated wave functions (dashed line)

and the one approximated by the Eq. (9). At $\eta = 0.01$, the extracted wave function agrees very well with the approximation, regardless of where in phase space region a mode is situated (Fig. 5(c)). In contrast, the mode in the chaotic region for $\eta = 0.1$ does not show a good agreement with the approximation, while the one in the regular region still abides by the aforementioned approximation (Fig. 5(d)). Of course, the disagreement is due to the level transitions during the dynamics.

Now, it is necessary to consider the general criteria for the variation of Born-Oppenheimer approximation[20, 21, 22], which is given as follows,

$$\hbar | \langle n | \dot{m} \rangle | \ll | E_n - E_m |. \quad (16)$$

This inequality simply guarantees that the heavy object is moving slowly enough to prevent level transitions. If we apply this inequality to our system, the condition of this inequality is not changed much by the dynamical status. In other words, the ratio between the left term and the right term in Eq.(16) is given as around 0.01 for $\eta = 0.01$ and around 0.2 for $\eta = 0.1$, no matter whether a mode is chaotic or regular.

Considering the near-integrability in the case of regular dynamics, it is obvious that the simple approximation works well in the regular region, because we can define good quantum numbers for each degree of freedom.

In addition, we can find the dynamical interpretation of the inequality (16). In our system, the satisfaction of (16) guarantees that the chaotic region is small enough in comparison to Planck’s constant \hbar . Therefore, it is

impossible that more than two modes are situated in the chaotic region. Accordingly, no transition is possible.

V. CONCLUSION

In this work, we study the validity of the Born-Oppenheimer approximation in the presence of chaotic dynamics. Especially, the criteria under which the approximation is working is interpreted from the dynamical point of view. We apply the approximation method to the autonomous Fermi accelerator which has a clear division of regular dynamics and chaotic dynamics in its phase space. In the regular region, the approximation is obviously well suited to calculate the eigenmodes, whereas it is just conditionally suited in the chaotic region. However, when the dynamics of the system satisfies the general condition for the approximation, that is, the evolution of the system is slow enough to prevent the level transitions, the area of the chaotic region becomes small enough in comparison to Planck's constant. Thus, the chaotic dynamics can not be resolved by wave functions. Thereby, the Born-Oppenheimer approximation can approximate the wave functions very well in spite of the chaotic nature of the dynamics.

It is important to remark that in the region where the Born-Oppenheimer approximation is working, we can apply another approximation to our system. Then we can follow the procedure of Ref. [19] to construct the density matrix and the reduced density matrix of the interesting subsystem (light particle or oscillating wall). We leave this for a future work. We also remark that it would be quite instructive to study higher order corrections to the Born-Oppenheimer approximation [20, 21] in connection with chaotic dynamics. We also leave this for a future study.

This work was supported in part by the Max-Planck-Institute for the Physics of Complex Systems (MPIPKS) in Dresden, the Emmy-Noether-Programme of the DFG (Germany) and by the Brazilian agencies, CNPq and FAPESP.

-
- [1] M. Born and V. Fock, Z. Phys. **51** 165 (1928).
 - [2] Jie Song *et al.*, Euro. Phys. Lett., **80**, 60001; A. M. Childs *et al.*, Phys. Rev. A **65** 012322 (2002).
 - [3] K. Marzlin and B. Sanders, Phys. Rev. Lett. **93**, 160408 (2004).
 - [4] D. M. Tong, K. Singh, L. C. Kwek and C. H. Oh, Phys. Rev. Lett. **98**, 150402 (2005).
 - [5] A. J. Lichtenberg and M. A. Lieberman, “*Regular and Stochastic Motion*”, (Springer-Verlag, Newyork, 1983).
 - [6] E. Fermi, Phys. Rev. **75**, 1169 (1949).
 - [7] S. Ulam, in “*Proc. 4th Berkeley Symposium on Mathematics and Probability 3*” 315, (Berkeley, Los Angeles, 1961).
 - [8] F. Lenz, F. K. Diakonov, and P. Schmelcher, Phys. Rev. Lett. **100**, 014103 (2008).
 - [9] R. Blümel and B. Esser, Phys. Rev. Lett. **72**, 3658 (1994).
 - [10] P. Seba Phys. Rev. Lett. **41**, 2306 (1991).
 - [11] F. Saif, I. Bialynicki-Birula, M. Fortunato, and W. P. Schleich, Phys. Rev. A **58**, 4779 (1998).
 - [12] F. R. N. Kock, F. Lenz, Christoph Petri, F. K. Diakonov, and P. Schmelcher, Phys. Rev. E. **78**, 056204 (2008).
 - [13] F. Marquardt, J. G. E. Harris, and S. M. Girvin, Phys. Rev. Lett. **96**, 103901 (2006).
 - [14] A. Steane, P. Szriftgiser, P. Desbiolles, and J Dalibard, Phys. Rev. Lett. **74**, 4972 (1995).
 - [15] L. D. Pustyl'nikov, Russian Math. Surveys **50**:1 145 (1995).
 - [16] A. C. J. Luo and Y. Guo, Mathematical Problems in Engineering. **2009**, Article ID 298906 (2009).
 - [17] G. M. Zaslavsky, R. Z. Sagdeev, D. A. Usikov and A. A. Chernikov, “*Weak Chaos and Quasi-Regular Patterns*”, (Cambridge University Press, 1991).
 - [18] Ramdas Ram-Mohan, “*Finite Element and Boundary Element Applications in Quantum Mechanics*”, (Oxford University Press, USA, 2002).
 - [19] M. S. Hussein and V. Kharchenko, Ann. Phys. **250**, 352 (1996).
 - [20] A. Mostafazadeh, Phys. Rev. A, **55**, 1653 (1997).
 - [21] R. Mackenzie, E Marcotte and H. Paquette, Phys. Rev. A **73**, 042104 (2006).
 - [22] Alfred Shapere and Frank Wklczek, “*Geometric Phases in Physics*”, (World Scientific, Singaport, 1989).